JOURNAL OF MATERIALS SCIENCE **39** (2004) 61 – 65

A study on the hydriding-dehydriding kinetics of $Mg_{1.9}Al_{0.1}Ni$

QIAN LI, QIN LIN, KUO-CHIH CHOU
Department of Physical Chemistry, University of Science and Technology Beijing, Beijing 100083, People's Republic of China
E-mail: lq75@263.net

LIJUN JIANG
Research Center of Energy Materials and Technology, General Research Institute for Nonferrous Metal, Beijing 100088, People's Republic of China

---

The hydrogen absorption/desorption (A/D) kinetics of hydrogen storage alloys $Mg_{1.9}Al_{0.1}Ni$ prepared by hydriding combustion synthesis in two-phase (α-β) region in the temperature range from 523 to 573 K have been investigated. The hydriding/dehydriding (H/D) reaction rate constants were extracted from the time-dependent A/D curves. The obtained hydrogen A/D kinetic curves were fitted using various rate equations to reveal the mechanism of the H/D processes. The relationships of rate constant with temperature were established. It was found that the three-dimensional diffusion process dominated the hydrogen A/D. The activation energies of $Mg_{1.9}Al_{0.1}Ni$ are 52 ± 2 and 48 ± 1 kJ/mol H_2 for the H/D processes smaller than that of Mg_2Ni, which can be explained that the improvement of H/D reaction kinetics in Mg_2Ni by using additive Al.

---

1. Introduction

Magnesium and magnesium alloys have been investigated as hydrogen storage materials for several decades because they store far more hydrogen by weight than most of the other currently known metal hydrides. However, these materials are plagued by poor A/D rates and are too stable for most practical application. Storage capacity and fast reaction rate are the most important properties for hydrogen storage alloys. Numerous experiments have therefore been performed to test the kinetics of various storage alloys, and much research has been carried out to improve the kinetic properties of Mg-based alloys. The main approaches include: (1) adding alloying elements, such as Zr, Al, Co, Mn, Cu, Ni, Ca, Fe, etc. [1–3]; (2) modifying the surface of the alloys by coating with metals such as Ni and Cu [4], or fluoride treatment [5]; (3) using novel methods, such as hydriding combustion synthesis (HCS), mechanical alloying (MA), to prepare alloys with amorphous microstructure and/or nanocrystalline [6]; (4) forming composites with other hydrogen storage alloys, such as nano-phase composite hydrogen storage alloys of Mg and $MmNi_{5-x}(CoAlMn)_x$ [7].

The reaction kinetics is greatly influenced by temperature, pressure and surface poisoning of Mg, various results were obtained and different interpretations were given [8–14]. Previous works show that the overall reaction of hydride formation/decomposition is composed of several steps, involving hydrogen dissociation and chemisorption on the surface, surface penetration by H atoms, hydrogen diffusion in the α or β phase and motion of the α/β interface. If one of these steps is very slow, it becomes the rate-controlling step and the kinetics of the overall process can be described by simple rate expressions [14, 15].

The usual method used to study kinetics is to fit the time-dependent transformed fraction $\alpha(t)$ with various analytical rate expressions, so as to identify the reaction mechanism or the intrinsic rate-limiting step. There is no report about the hydrogen A/D kinetics of $Mg_{1.9}Al_{0.1}Ni$ alloy. The primary concern in this study was to get the kinetic data at completely isothermal conditions. The experiments were carried out with a small amount of $Mg_{1.9}Al_{0.1}Ni$ at relatively low initial hydrogen pressure to reduce the liberation of reaction heat and the rate. The reactor was especially designed to achieve good heat transfer and immersed in a constant temperature electric furnace, the hydrogen A/D kinetics in the two-phase (α-β) coexistence region was investigated systematically. The kinetic mechanism of hydrogen A/D reaction was studied and the kinetic parameter was determined by comparing the experimental results with the 42 reaction functions [16, 17]. The experimental results fitted well with analytical equations. Based on data analysis, a preliminary explanation of the experimental results is given.

2. Experimental details

2.1. Kinetic measurement of hydrogen absorption and desorption

The alloy used in this study was prepared by combustion synthesis in our previous work [18]. The experimental

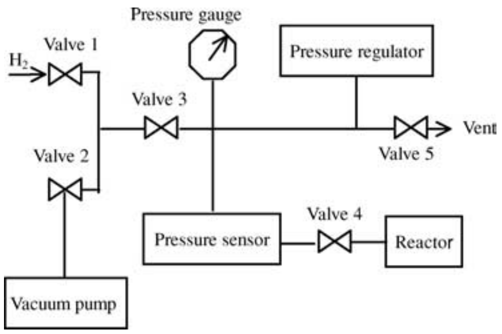

Figure 1 The schematic diagram hydride kinetics apparatus.

apparatus used to prepare the hydride and perform kinetics measurements is shown schematically in Fig. 1. It consisted of a stainless steel manifold with ports for adding hydrogen, venting and evacuating system. An electric furnace with designed constant temperature was used to keep the sample at constant temperature within ±2 K and a thermocouple with 0.85 mm diameter was used to measure the temperature accurately. $Mg_{1.9}Al_{0.1}Ni$ powder weighing 0.5 g was used in order to reduce the generation of the reaction heat.

In order to measure the kinetics of hydrogen absorption accurately, the sample was evacuated to 0.133 Pa for 1 h to remove any gas in the system. Then valves 2, 4 were closed, the rated hydrogen was introduced to the system immediately. With the help of a manually operated needle valve 3 the rated hydrogen introduced to the reactor till the hydrogen pressure reached the point (P_1 as shown in Fig. 2) in the α-β phase. Then, the reaction rates were measured by the method of initial rates in small concentration steps in the two-phase region as shown in Fig. 2. A small amount of hydrogen of purity 99.999% with the pressure P was introduced into the reactor. The sudden pressure drops from P to P_0, the reacting initial pressure is caused by the volume increase of the reaction system. The real pressure drop due to the hydrogen absorption was started from P_0 to P_{eq} in the closed system. The magnitude of pressure drop was monitored at regular time intervals. During the measurement for the kinetics of hydrogen desorption, the sample was charged with given amount hydrogen at each temperature in order to keep it in suitable situation (e.g., as H_4 in Fig. 2.). Then valve 4 was closed and valves 2, 3 were opened to evacuate the system for obtaining a lower pressure of 0.133 Pa (much below the hydride decomposition pressure, as P'_0 in Fig. 2). The hydride sample was suddenly exposed to a lower pressure with the help of a manually operated needle valve. This exposure of the charged sample to the low pressure resulted in release of hydrogen from the sample causing a pressure rise from P'_0 to P_{eq} in the closed system. The magnitude of pressure rise was monitored at regular time intervals.

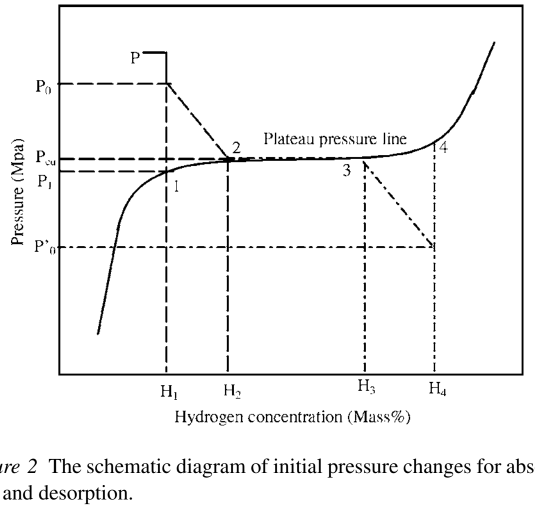

Figure 2 The schematic diagram of initial pressure changes for absorption and desorption.

2.2. Kinetic equation

Usually the rate equation of kinetics for solid-gas reaction was expressed as following:

$$\frac{d\alpha}{dt} = k \cdot f(\alpha) \tag{1}$$

where α is the reacted fraction at time t; k is rate constant; $f(\alpha)$ is function determining the mechanism of reaction and $g(\alpha)$ is the integral form of $f(\alpha)$, i.e.,

$$g(\alpha) = \int \frac{d\alpha}{f(\alpha)} = kt \tag{2}$$

$f(\alpha)$ or $g(\alpha)$ stand for the 42 mechanism functions representing chemical reaction, diffusion, nucleation and nuclei growth respectively (Table I).

Based on experimental data of hydrogen A/D curves, the reacted fraction α can be calculated, $\alpha = (P_0 - P_t)/(P_0 - P_{eq})$. P_0 is the initial pressure of the reaction. P_t and P_{eq} are the pressures of time t and finial equilibrium respectively. The data of t, α and $(d\alpha/dt)$ obtained from α-t kinetic curves of hydrogen A/D were regressed linearly by computer based on the Equations 1 and 2. The function $f(\alpha)$ or $g(\alpha)$ giving the best linearity is considered as mechanism of hydrogen A/D reaction in the alloy. The rate equation of H/D reaction and the kinetics parameters k can be obtained.

3. Results and discussion

The PC-isothermal curves in the temperature range from 523 to 623 K of $Mg_{1.9}Al_{0.1}Ni$ were reported by Li *et al.* [18]. It shows that the plateau region is relatively flat. The hydrogen absorption plateau pressures noted at a fixed hydrogen concentration of 1.5 mass% H were 1.098, 0.293 and 0.132 MPa and that of hydrogen desorption were 0.722, 0.162 and 0.071 MPa at 623, 553 and 523 K, respectively. These pressure values are very close to the values obtained by mimetic measurements, which are discussed below. The kinetic data of hydrogen A/D for the two-phase (α-β) region $Mg_{1.9}Al_{0.1}Ni$ at different temperatures were obtained at a rated hydrogen concentration about 1.5 mass% H.

Figs 3 and 4 show the representative H/D curves in the two-phase (α-β) region at different temperatures. Compared these curves, it is known intuitively that the higher the temperature of the system, the faster the hydriding and reaction rate are. It took 100 s for the transformed

TABLE I Mechanism function of the kinetics

Mechanism	$f(\alpha)$	$g(\alpha)$	r
Nucleation and growth	$(1/r)(1-\alpha)[-\ln(1-\alpha)]^{1-r}$	$[-\ln(1-\alpha)]^{r}$	1/4, 1/3, 2/5, 1/2, 2/3, 3/4, 1, 3/2, 2, 3, 4
Power law	$(1/r)\,\alpha^{1-r}$	α^{r}	1/4, 1/3, 1/2, 1, 3/2, 2
Exponential	$(1/r)\,\alpha$	$\ln \alpha^{r}$	1, 2
Branching nucleation	$\alpha(1-\alpha)$	$\ln[\alpha/(1-\alpha)]$	
Phase boundary reaction	$(1-\alpha)^{r}/(1-r)$	$1-(1-\alpha)^{1-r}$	1/2, 2/3
Chemical reaction	$(1/r)\,(1-\alpha)^{r}$	$1-(1-\alpha)^{r}$	1/2, 2, 3, 4, 1/4, 1/3
	$(1/2)(1-\alpha)^{3}$	$(1-\alpha)^{-2}$	
	$(1-\alpha)^{2}$	$(1-\alpha)^{-1}-1$	
	$2(1-\alpha)^{3/2}$	$(1-\alpha)^{-1/2}$	
	$(1/2)(1-\alpha)^{-2/3}$	$(1-\alpha)^{-1}$	
1-dimensional diffusion	$(1/2)\,\alpha^{-1}$	α^{2}	
2-dimensional diffusion	$[-\ln(1-\alpha)]^{-1}$	$\alpha+(1-\alpha)\ln(1-\alpha)$	
	$(1-\alpha)^{1/2}[1-(1-\alpha)^{1/2}]^{-1}$	$1-(1-\alpha)^{1/2}]^{2}$	
	$4(1-\alpha)^{1/2}[1-(1-\alpha)^{1/2}]^{1/2}$	$[1-(1-\alpha)^{1/2}]^{1/2}$	
3-dimensional diffusion	$(3/2)(1-\alpha)^{2/3}[1-(1-\alpha)^{1/3}]^{-1}$	$[1-(1-\alpha)^{1/3}]^{2}$	
	$6(1-\alpha)^{2/3}[1-(1-\alpha)^{1/3}]^{1/2}$	$[1-(1-\alpha)^{1/3}]^{1/2}$	
	$(3/2)[(1-\alpha)^{-1/3}-1]^{-1}$	$1-2\alpha/3-(1-\alpha)^{2/3}$	
	$(3/2)(1+\alpha)^{2/3}[(1+\alpha)^{1/3}-1]^{-1}$	$[(1+\alpha)^{1/3}-1]^{2}$	
	$(3/2)(1-\alpha)^{4/3}[(1-\alpha)^{-1/3}-1]^{-1}$	$[(1-\alpha)^{(-1/3)}-1]^{2}$	
		$(1+\alpha)^{2/3}+(1-\alpha)^{2/3}$	

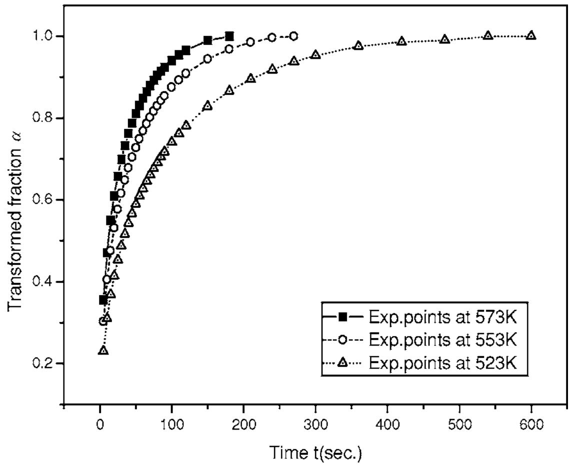

Figure 3 Hydrogen absorption curves in the two-phase (α-β) region of $Mg_{1.9}Al_{0.1}Ni$ at different temperatures.

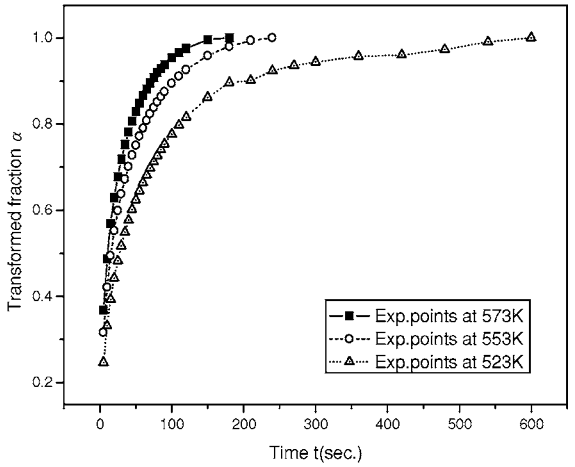

Figure 4 Hydrogen desorption curves in the two-phase (α-β) region of $Mg_{1.9}Al_{0.1}Ni$ at different temperatures.

fraction to reach 0.94 and 0.88 in the two-phase (α-β) region for 573 and 553 K, respectively. Compared with the experimental data of hydrogen A/D under the same temperature, it is found that the dehydriding reaction rate is slight faster than the hydriding rate. It took 100 s to 0.88 and 0.90 of the reacted fraction at 553 K for H/D processes.

In parallel with the change of H/D kinetics with increasing temperature, the shape of the H/D curves don't change. This is most likely associated with no changes in the rate-limiting step for A/D. Usually, the reaction mechanism can be analyzed by comparing the observed H/D rate curve with the rate equations derived from different processes, such as nucleation and growth process, auto-catalytic reactions, phase-boundary-controlled reactions and so on. Some rate equations proposed in the literature [19–21] have been used to treat the experimental data, but the fittings were very bad.

In order to more clearly study the mechanism of the hydrogen A/D, the individual curve was divided into the prophase and the anaphase. The hydrogen absorption curves in the two-phase (α-β) region from 523 to 573 K can be fitted with good accuracy by Jander diffusion model in Fig. 5, which is the rate expression $[1-(1-\alpha)^{1/3}]^2 = kt$. The same phenomenon existed

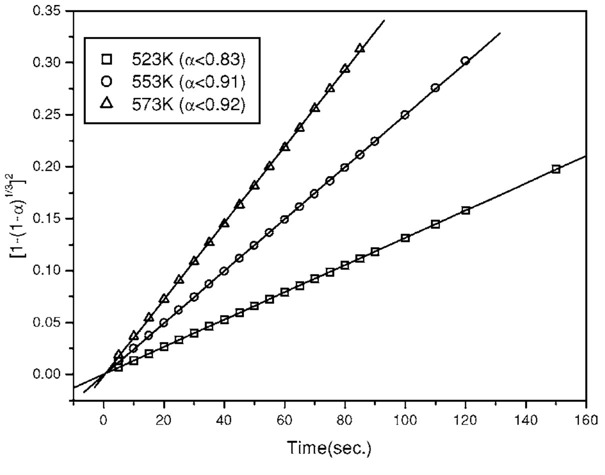

Figure 5 Plot of $[1-(1-\alpha)^{1/3}]^2$ vs. time for hydriding reaction of the two-phase (α-β) region of $Mg_{1.9}Al_{0.1}Ni$ at different temperatures.

TABLE II Kinetic parameters, equation and activation energies for hydriding/dehydriding reaction under different conditions

	Hydriding process			Dehydriding process		
T (K)	523 (α < 0.83)	553 (α < 0.91)	573 (α < 0.92)	523 (α < 0.86)	553 (α < 0.94)	573 (α < 0.95)
Best fitting equation		$[1-(1-\alpha)^{1/3}]^2$			$[1-(1-\alpha)^{1/3}]^2$	
Rate constant (10^3 s^{-1})	1.31	2.50	3.68	1.55	2.79	4.07
Correl. coef.	0.9999	0.9999	0.9999	0.9999	0.9999	0.9998
Rate-limiting step		Three-dimensional diffusion			Three-dimensional diffusion	
Activation energy (kJ/mol)		52 ± 2			48 ± 1	

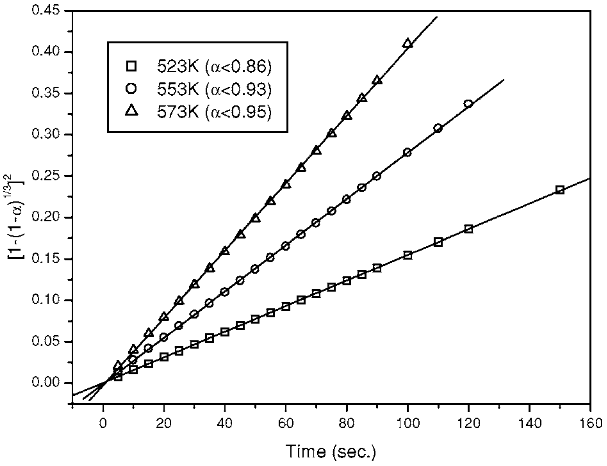

Figure 6 Plot of $[1-(1-\alpha)^{1/3}]^2$ vs. time for dehydriding reaction of the two-phase (α-β) region of $Mg_{1.9}Al_{0.1}Ni$ at different temperatures.

in the hydrogen desorption process in the temperatures range from 523 to 573 K, as shown in Fig. 6. It is suggested that the rate-limiting steps of the H/D process followed the same kinetic mechanism, which was three-dimensional diffusion of hydrogen atoms through the hydride phase (β phase) in the hydriding process and the diffusion of hydrogen in the α solid solution in the dehydriding process.

When the rate constants at various temperatures were extracted from the hydrogen A/D curves, it was possible to construct the Arrhenius plots in Fig. 7. The apparent activation energies of 52 ± 2 and 48 ± 1 kJ/mol H_2 for the H/D processes in the tow-phase (α-β) coexistence region from 523 to 573 K were obtained, respectively.

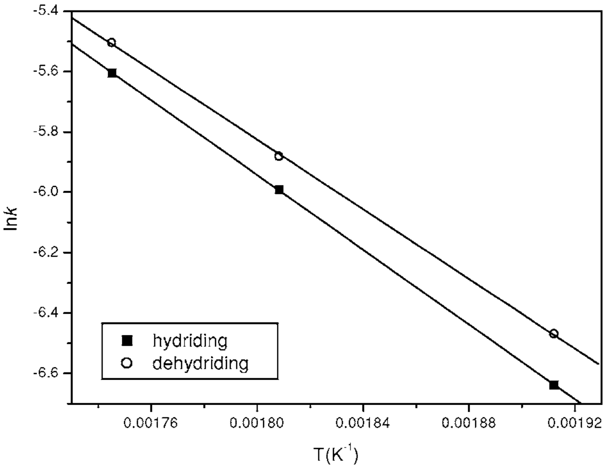

Figure 7 Arrhenius plot of hydriding/dehydriding reaction rate in the two-phase (α-β) region of $Mg_{1.9}Al_{0.1}Ni$.

All rate constants of individual phase in the H/D reaction were summarized in Table II including correlation coefficient, the corresponding kinetic function and activation energies. It is well known that the smaller the activation energy, the larger the rate constant and the faster the reaction rate are. Compared to these values, it was found that the activation energy of hydrogen absorption was larger than that of dehydriding reaction in $Mg_{1.9}Al_{0.1}Ni$, the rate constants of the former were smaller than these of the later. It can be concluded that the reaction rate of the dehydriding process is faster than that of the hydriding process in the two-phase (α-β) region in the temperature range from 523 to 573 K.

The apparent activation energy for the diffusion-controlled hydrogen absorption was determined to be 52 ± 2 kJ/mol in the temperature range from 523 to 573 K, which is much smaller than that (64 kJ/mol) of Mg_2Ni prepared by hydriding combustion synthesized [22]. This may be due to the high diffusivity of hydrogen in the hydride forming metals, which diffusivity exceeds that of heavy interstitials by many orders of magnitude [23]. Han [24] reported that the rate-controlling step of the dehydriding reaction in Mg_2Ni was the diffusion of hydrogen in the α phase and the apparent activation energy of the dehydriding reaction of Mg_2Ni was 62 kJ/mol, which is larger than that of $Mg_{1.9}Al_{0.1}Ni$ (48 ± 1 kJ/mol) in this paper. It is revealed that the energy barrier to recombination desorption is deduced by adding Al to Mg_2Ni with no change of the kinetic mechanism. It is reasonable to explain that the hydriding kinetics of Mg_2Ni was improved by using additive Al.

4. Conclusion

Hydrogen absorption and desorption kinetics were investigated in $Mg_{1.9}Al_{0.1}Ni$ alloy in the temperature range from 523 to 573 K under isothermal condition. The obtained kinetic curves were fitted using various rate equations derived from different kinetic reaction process. It was found that the H/D kinetics in the two-phase (α-β) region were all well in agreement with the Jander rate equation, $[1-(1-\alpha)^{1/3}]^2 = kt$, the three-dimensional diffusion process. The apparent activation energies were determined to be 52 ± 2 and 48 ± 1 kJ/mol H_2 for the H/D processes in the two-phase (α-β) region from 523 to 573 K were obtained, respectively, which were smaller than these of Mg_2Ni in the same range of temperature. It can be explained that the improvement of H/D reaction kinetics in Mg_2Ni by using additive Al.

Acknowledgements

This research was supported by the Ministry of Science and Technology of China. (Grant No. 2000 026405).

References

1. Y. TSUSHIO and E. AKIBA, *J. Alloys Comp.* **267** (1998) 246.
2. R. L. HOLTZ and M. A. IMAM, *J. Mater. Sci.* **34** (1999) 2655.
3. *Idem.*, *ibid.* **32** (1997) 2267.
4. J. L. LUO and N. CUI, *J. Alloys Comp.* **288** (1999) 286.
5. C. Y. WANG, P. YAO and D. H. BRADHURST, *et al.*, *ibid.* **285** (1999) 267.
6. L. ZULUSKI, A. ZALUSKA and J. O. STROM-OLSEN, *ibid.* **217** (1995) 295.
7. M. ZHU, Y. GAO, X. Z. CHE, *et al.*, *ibid.* **330/333** (2002) 708.
8. A. S. PERDERSOM, K. JENSEN, B. LARSEN, *et al.*, *J. Less-Common Met.* **131** (1987) 31.
9. J. M. BOULET and N. GERARD, *ibid.* **89** (1983) 151.
10. A. S. PERDERSOM, K. JENSEN, B. LARSEN, *et al.*, *Int. J. Hydrogen Energy* **8** (1983) 205.
11. L. BELKBIR, E. JOLY and N. GERARD, *ibid.* **6** (1981) 285.
12. E. AKIBA, K. NOMORA, S. ONO, *et al.*, *ibid.* **7** (1982) 787.
13. M. Y. SONG, J. P. MANAUD and B. DARRIET, *J. Alloys Comp.* **282** (1999) 243.
14. M. MARTIN, C. GOMMEL, C. BORKHART, *et al.*, *ibid.* **238** (1996) 193.
15. X. H. WANG, C. S. WANG, C. P. CHEN, *et al.*, *Int. J. Hydrogen Energy* **21** (1996) 479.
16. LIN QIN, CHEN NING, YE WEN, *et al.*, *J. Univ. Sci. Tech. Beijing* **4**(2) (1997) 34.
17. LI WENCHAO, "The Kinetics of Metallurgy and Materials," (Academic press, Beijing, 2001) p. 346.
18. LI QIAN, JIANG LIJUN, LIN QIN, KUO-CHIH CHOU, *et al.*, *The Chinese J. Nonferr. Met.* **13**(4) (2003) 864–870.
19. G. LIANG, J. HOUT, S. BOILY, *et al.*, *J. Alloys Comp.* **305** (2000) 239.
20. W. ZHANG, J. CIMATO and A. J. GOUDY, *ibid.* **201** (1993) 176.
21. M. N. MUNGOLE and R. BALASUBRAMANIAM, *Int. J. Hydrogen Energy* **23** (1998) 349.
22. LI QIAN, LIN QIN, JIANG LIJUN, *et al.*, *J. Mate. Sci. Tech.* (in press).
23. M. H. MINTZ, *J. Bloch, Prog. Solid State Chem.* **16** (1985) 163.
24. JEONG SEB HAN and JAI-YOUNG LEE, *J. Less-Common Met.* **128** (1987) 155.

Received 1 July
and accepted 25 August 2003